OPEN ACCESS
SPIN
(2024) 2450020 (8 pages)

DOI: 10.1142/S2010324724500206

World Scientific
www.worldscientific.com

Fingerprinting Magnetic States in Interconnected Nanoring Arrays via Spin Wave Spectra

C. Swindells*, D. R. Eade, T. Silsupadol and T. J. Hayward
School of Chemical, Materials and Biological Engineering
University of Sheffield, S1 3JD, UK
**c.swindells@sheffield.ac.uk*

Received 12 June 2024
Accepted 22 September 2024
Published 21 November 2024

Arrays of interconnected magnetic nanorings show emergent dynamics arising from stochastic interactions at junctions between rings. These global emergent properties have already shown potential as a platform for reservoir computing. However, their experimental computational performance has been limited by the use of a single-dimensional global measurement, their magnetoresistance, as an output, masking much of the underlying state information. Here, we show in both simulation and experiment the potential of using the spin wave spectra of such arrays of nanorings to produce a fingerprint of the number and orientation of the internal magnetic states, providing a route towards a multi-dimensional output with which to perform computation. We show that the spectra fulfill the two criteria for reservoir computing: a nonlinear response to an input stimulus, and a fading memory.

Keywords: Spin wave; nanoring; micromagnetics; ferromagnetic resonance; reservoir computing.

1. Introduction

Neuromorphic computing on conventional silicon hardware is incredibly inefficient, with substantial energy costs in shuffling data between memory and processing units, a barrier known as the von Neumann bottleneck.[1] With the rise in machine learning, this problem has been amplified, with large amounts of energy required to train weights between nodes in commonly used recurrent neural networks. Reservoir Computing (RC) offers a potential solution, in which a recurrent network, where all internal connections are trained, is replaced by a dynamic system, where only the output layer is trained.[2,3] Further energy savings can be found by replacing the dynamic system in software with a material platform, where the inherent complex physics provides a suitable transform to encoded data. This approach requires methods of interfacing with materials for data output, which not only provide substantial information regarding the state of the system, but are also energy efficient.

Material systems must fulfill two broad criteria to be considered as RC platforms; a measurable nonlinear response to an input stimuli, and a dependence of the current system state upon previous states that asymptotically reduces over time, often termed 'fading memory'. In recent years, several

*Corresponding author.

material platforms have been proposed which meet these criteria, not limited to memristors,[4,5] photonic,[6,7] and magnetic systems.[8,9] Magnetic materials in particular are ideal candidates for in-materio RC devices due to their underlying inherent nonlinearity and hysteretic properties. Competitive computational performance has already been shown in a host of magnetic and spintronic systems including spin-oscillators,[10,11] skyrmions,[12,13] spin ices[14,15] and domain walls in nanowires.[16] Recently, we have demonstrated that the domain wall population of an array of interconnected magnetic rings driven by a rotating magnetic field has been proposed to be an emergent property and proposed to be a possible substrate for performing RC.[17] We have shown the capability of such an ensemble at performing a range of benchmark tasks and reservoir configurations.[18,19] However, a common problem with magnetic RC platforms are methods of measuring the states of complex systems in sufficient detail for a meaningful output, which do not mask the richness of the system's internal states.[20] In these proto-devices of nanorings, the system state was probed using magnetoresistance, providing only a single-dimensional representation of the complex magnetic state of the arrays to be used as an output to train on, thus limiting their potential as in-materio computing devices.

Spin waves have long been proposed as an efficient alternative information carrier in next generation devices, and have recently been demonstrated as capable platforms for in materio computing in systems including magnonic crystals[21,22] and artificial spin ice arrays.[14,23] In demonstrations of computation with spin ices, the spin-wave spectra provided information on the rich variety of internal system states with frequency binning of the spectra providing a multi-dimensional output upon which to train on.[15] Though the spin wave spectra of individual[24] and coupled[25,26] nanorings have been reported, it remains an open question whether the spectra can provide enough state information in arrays of nanorings, where the emergent properties of domain wall interactions at junctions perform useful computation.

In this work we show in both simulation and experiments that the spin wave spectra can be used as a proxy for information about the orientation and numbers of states within a nanoring ensemble. We observe that system has both a nonlinear response of the spectra to an input stimulus in the form of a rotating magnetic field, and a transient change in the spectra between inputs. This fulfils the two broad criteria for RC, a key first step to utilizing the spin-wave spectra as a viable readout method.

2. Simulation and Experimental Details

Micromagnetic simulations of nanorings were performed using the MuMax3 package.[27] For these simulations, a 2×2 array of rings was used, with the ring diameter $4\,\mu$m, the track width 400 nm, and the thickness 10 nm. Overlap between the rings was 50% and periodic boundary conditions were in place on all sides. The cell size in X and Y was set to 5 nm and 10 nm in Z. Typical NiFe material parameters were used:[28] saturation magnetization of 860 kA/m, exchange stiffness of 13×10^{-12} J/m, and damping of 0.007.

To simulate the frequency response of the array, a broadband 50 GHz *sinc* pulse with amplitude 1 Oe was applied in the x-direction, delayed by 20 ns. Simulations were run for 60 ns, recording the magnetization components at 12 ps intervals. The resulting simulated frequency-space spectra were then determined through the Fourier transform of the M_z component of the transient magnetization response.

Nanoring ensembles for ferromagnetic resonance measurements were patterned using electron beam lithography with a Raith Voyager system, with Permalloy (NiFe) films deposited using thermal evaporation. Samples were fabricated in a regular square grid, covering a 2×12 mm area where each ring had a $4\,\mu$m diameter, track widths of 400 nm, 50% overlap between neighboring rings and a thickness of 30 nm.

To set the state of the array, a rotating magnetic field was applied achieved using a pair of electromagnetic coils. Following the application of the field, microwave measurements were then undertaken with the sample placed face down on a coplanar waveguide, and the RF excitation frequency swept, with the resulting RF power measured using a diode. To improve signal to noise, the pair of coils orthogonal to the RF field was used to apply a small (sub 10 Oe) 1 kHz AC field, allowing for lock-in detection.

3. Magnetic Ring States

Interconnected ring arrays can form a multitude of complex magnetization states, with examples

illustrated in Fig. 1. These can be broken down into a number of elemental metastable states of the individual rings, which can be categorized depending on the number of domain walls in the ring.[29,30] Onion states within the rings have a net magnetization where regions are separated by domain walls, as shown in Figs. 1(a) and 1(d). Vortex states contain no domain walls, have circumferential magnetization and provide no net magnetic moment. Vortex states in adjacent rings typically have opposite circulation (clockwise/anticlockwise) to avoid magnetic frustration (Fig. 1(b)).

Domain walls will rotate around the ring with a sufficiently strong rotating magnetic field. The presence of the junction between rings presents an energy barrier to the movement of domain walls.[31] As a rotating magnetic field is applied, stochastic domain wall annihilation and creation processes can occur, depending upon the strength of the field.[19] At low magnetic fields, domain walls will propagate around the ring, becoming pinned at the junction, while at sufficiently high fields, domain walls will follow the applied clocking field without pinning at the junctions. In between these regimes, the domain walls will probabilistically pin and de-pin, annihilate one another and respawn, producing vortex states, and onion states in varying orientations, and states with one displaced domain walls, termed 3/4 states, an example of which is shown in Fig. 1(c).

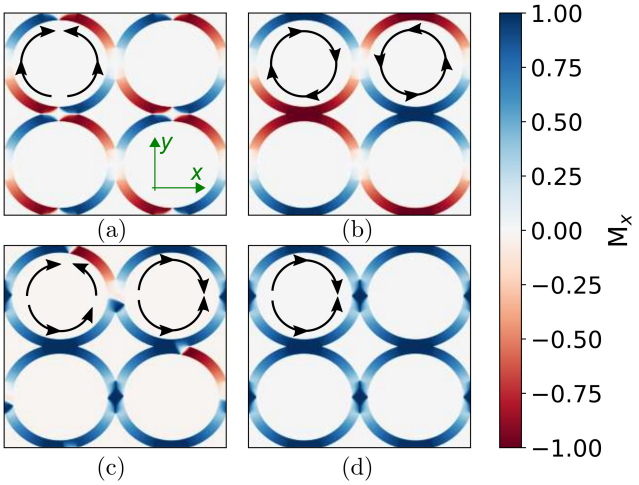

Fig. 1. Simulated states of a 2×2 array of rings, showing (a) onion states with domain walls at junctions aligned in the y-direction, (b) pairs of clockwise and anti-clockwise vortex states with no domain walls, (c) 3/4 states in two of the rings, with additional domain walls and (d) onion states aligned in the x-direction. Arrows provide a guide to the direction of magnetization.

4. Static State Spin Wave Spectra

Though the magneto resistance response has successfully been shown to be used as an output to competitive performance in benchmark machine learning tasks,[19] this approach is limited in that a single global response of the system is measured, which masks the underlying complexity from the rich state space detailed in the previous section to a single resistance value.

An alternative output method is to measure the spin-wave spectra of the system, providing a multi-dimensional output in the form of bins in frequency space. This has already been shown to provide a large degree of system information within spin ice systems.[15] The shape anisotropy of nanoscale ring arrays should allow for field-free resonances, the frequency of which will depend upon the structural parameters, (such as the ring diameter), while the measured RF absorption should depend on both the number of vortex states and the number and relative orientation of onion and 3/4 states, with respect to orientation of the field from RF excitation.

Prior to the use of the spin-wave spectra for computation, the steady-state frequency response arising from ring states must be shown to provide sufficiently distinct outputs with changes to the internal system state. Simulated frequency spectra for each of the states described in Fig. 1 are shown in Fig. 2.

The magnitude of the peaks of the spectra obtained from the vortex states, and for the onion states aligned with RF excitation are minimal

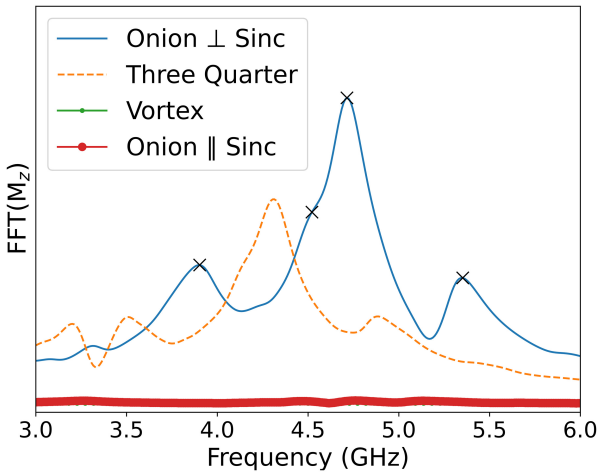

Fig. 2. Fourier transform of the M_z component for each of the ring states shown in Fig. 1 following the application of a *sinc* pulse in the x-direction. Black crosses mark position of main modes identified.

compared to those from the onion states aligned orthogonal to the *sinc* pulse. This can be explained by considering the net effective moment of the total system, with respect to the direction of RF excitation. The torque on the magnetization depends on the direction of magnetization and the direction of the RF excitation. For the onion states orthogonal to the RF field, there is a large net moment which the excitation can exert a torque upon. In the case of the vortex states there is no net moment and no net torque from the RF. For the onions states aligned parallel to the excitation, there is a much smaller component orthogonal to the RF field, and hence minimal torque. For the system with two 3/4 states, there are still observable spectra but they are shifted to a lower frequency due to the lower effective magnetic moment, as would be expected from a Kittel-like relation.[32]

Where the onions states are aligned orthogonal to the RF excitation field, four peaks are observed, at 3.9 GHz, 4.5 GHz, 4.7 GHz and 5.4 GHz. To investigate which modes they correspond to, the *sinc* pulse was replaced by a constant frequency sine wave and the simulation re-ran, recording the state at 10 ps intervals. The evolution of the magnetization once a steady state had been reached is shown in Fig. 3. The difference in the M_z component between the maxima and minima of the sine-wave excitation in the final panel highlights the difference between the four modes. The first frequency primarily corresponds to a mode confined to the junctions of the ring. The second and third modes correspond to modes within the arms of the ring, with the 4.5 GHz mode also coupled to the state of the junction. The final mode is mainly in the upper and lower junctions of each ring where the domain wall is present.

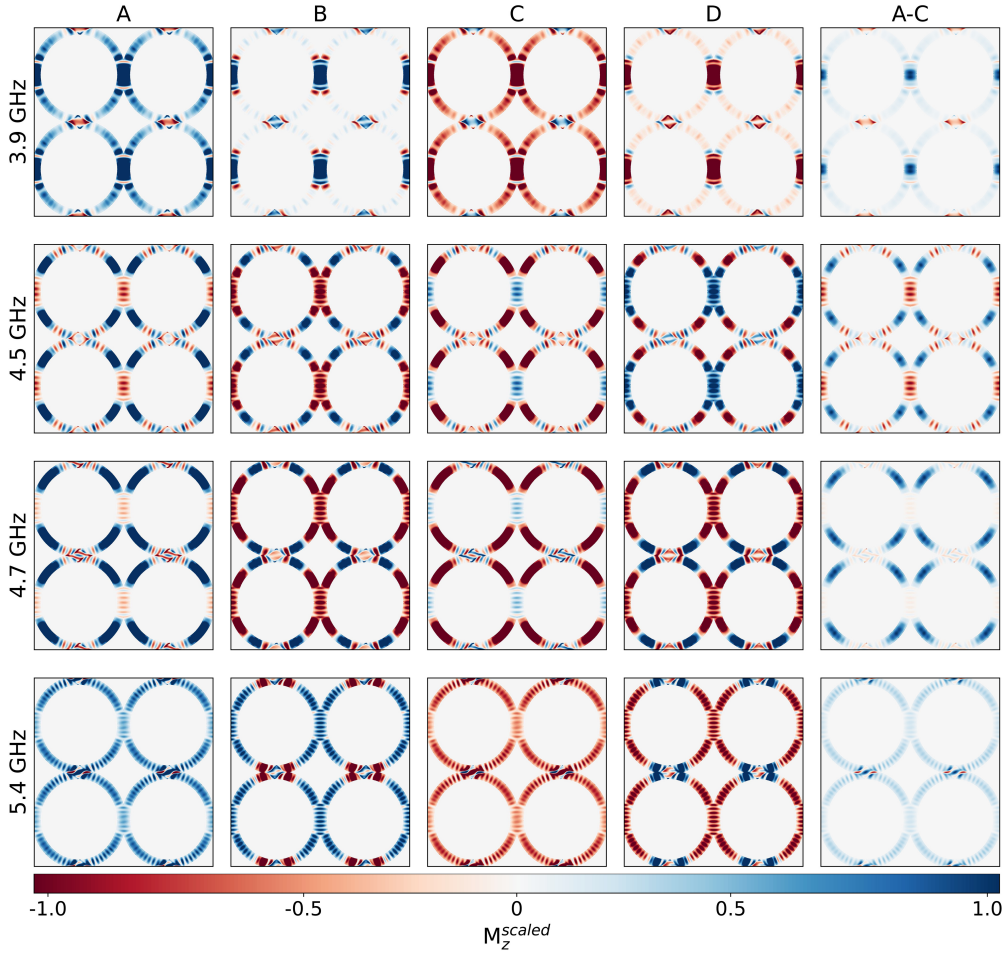

Fig. 3. Snapshots of the M_z component of an onion state as a sine wave microwave field is applied. The four frequencies shown correspond to the modes obtained in Fig. 2. Positions A and C correspond to the maxima and minima of the sine wave respectively, with B and D the crossing points. The final panel is the difference between the maxima and minima of the excitation, highlighting the dominant regions active.

5. Nonlinear Responses to Magnetic Field Amplitude

For nanoring ensembles, we have previously demonstrated that the region in which best computational performance is achieved is on the cusp of the emergent regime, where stochastic processes produce a variety of orientations of states.[17–19] While micromagnetic simulations have shown a difference in frequency response between different states, in order to be useful as a computational output for RC, the system must demonstrate a nonlinear variation of the output as a function of input stimulus. In the nanoring array, this should correspond to the difference in frequency response from the transition from onion states to vortices, 3/4 states and onion states no longer orthogonal to the RF excitation.

To experimentally probe the response of the ring array as a function of rotating field strength, the signal from the lock-in amplifier was recorded as a function of RF frequency, following the application of 200 cycles of a rotating magnetic field for the sample described in Sec. 2. The lock-in detection using field perturbation produces a derivative of the signal. The system was initialized such that the rings are set into onions orthogonal to the RF excitation. The magnetic field then was rotated such that the final applied field direction was orthogonal to the direction of RF excitation.

The steady-state response of the ring array was obtained after many rotations to wash out any transient response. The obtained spectra for varying rotating field strengths are shown in Fig. 4(a), with several, horizontal linescans shown in Fig. 4(b). Three distinct regimes are observed in the colorplot, corresponding to the those found previously in similar magnetoresistance measurements.[19] At low rotating fields, below 45 Oe in this case, the onion states remain pinned and aligned orthogonal to the RF excitation, resulting in a clear measurable signal. Above a threshold field, around 56 Oe, the domain walls propagate around the ring with the applied field, with sufficient energy to overcome the barrier at the junction. The final onion states are aligned orthogonal to the RF excitation, and hence the measured signal is identical to that at low fields. For a saturated state, four distinct modes are observed, aligning with those simulated in Fig. 3.

In between these two regimes, stochastic processes as domain walls enter junctions between rings leads to the formation of vortex states, 3/4 states, and onion states no longer orthogonal to the RF excitation. These additional states decrease the measured signal, as was expected from the simulated states in Fig. 2.

The nonlinear variation of the spin-wave spectra of the array as a function of input stimulus can be visualized by tracking the intensity of the signal from the lock-in amplifier for a fixed RF excitation frequency as a function of rotating field strength, as shown in Fig. 4(c). Nonlinear transforms are

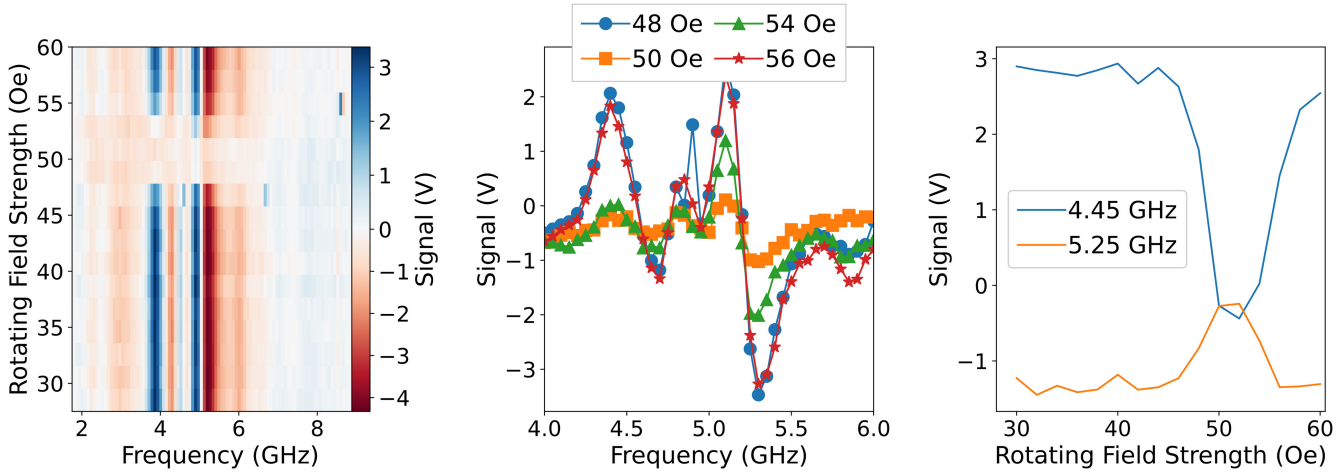

(a) (b) (c)

Fig. 4. Experimental data of a 400 nm width ring array, with (a) Frequency-swept ferromagnetic resonance scans as a function of rotating field after 200 cycles of constant field. (b) Linescans around the emergent regime, showing the loss of signal from the reduction of numbers of onion states orthogonal to the RF torque. (c) The recorded signal at two frequencies as a function of rotating field strength.

observed due to the changing relative numbers of states within the system. The spin-wave spectra obtained strongly depend on the direction of the net magnetization, for a fixed RF excitation direction, these spectra will allow for a fingerprinting of states, producing a multi-dimensional output through frequency binning; ideally suited for computational tasks.

6. Transient Dynamics

The final criteria for an in-materio RC platform is often termed 'fading memory'; where future states are dependent upon previous states, such that information provided to the system asymptotically fades as new information is provided. It has additionally been shown for arrays of nanorings that competitive computational performance is obtained by utilizing regimes of response in which the array state is in transience.[18,19] For the spin wave spectra to be a viable output method for in-materio computation, they must be able to capture the material response prior to reaching a steady-state level.

The transient states of the array were experimentally measured by recording the frequency response of the system upon successive rotations of a fixed magnetic field. Frequency scans of the cycle by cycle response for select numbers of rotations, at field of a 52 Oe, is shown in Fig. 5. Here, the measured spectra require multiple rotations of field to reach an equilibrium due to the stochastic nature of interactions of the domain walls at the junctions between overlapping rings, and the resulting emergent behavior across the array.

With successive field rotations within the emergent regime, the relative numbers of onion states orthogonal to the RF excitation are reduced in number, while the number of vortex, 3/4, and onion states aligned to the RF excitation increase. After 10 rotations, the highest frequency mode, corresponding to the junctions with domain walls present, is almost fully suppressed due to the change in state. Though the other modes are also reduced in magnitude, a signal is still measured due to the stochastic nature of domain wall interactions ensuring that the array is not in a state entirely filled with vortex pairs.

The rate of decay towards an equilibrium is also dependent upon the magnetic field amplitude and mode excited by the RF excitation. This is shown in Fig. 5(b), where the signal from the lock-in amplifier at a fixed frequency and field is measured as a function as the number of field rotations. For a given computational task, the decay rate of the array, and hence how long information is held in the array, could therefore be tailored to be faster or slower towards an equilibrium condition by varying the number of rotations per input. These complex transforms as a function of input cycles hold promise for the spin wave spectra of fulfilling the criteria of RC, i.e., fading memory.

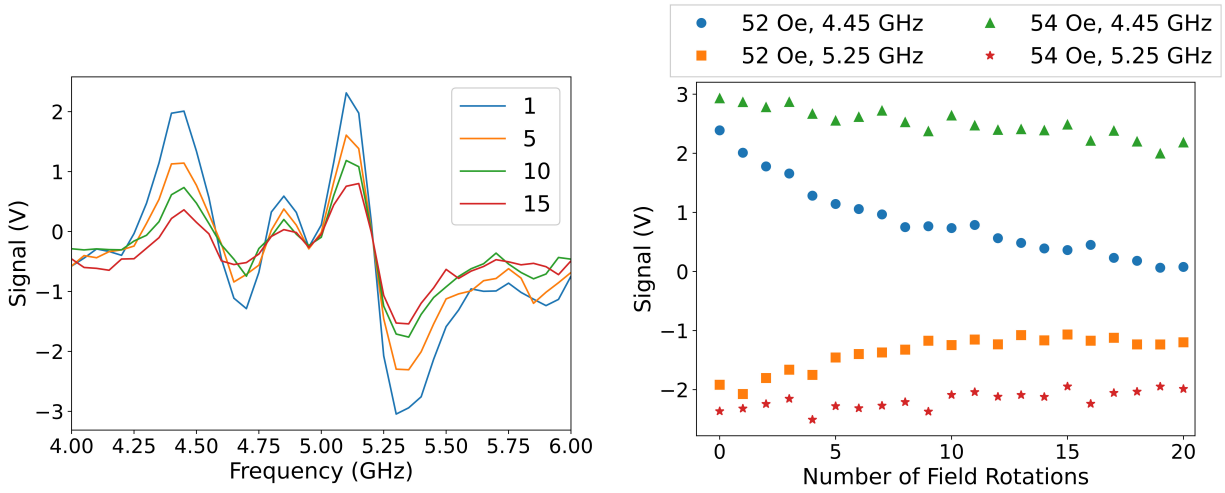

(a) (b)

Fig. 5. (a) The measured frequency response of the ring array following N cycles of a 52 Oe rotating magnetic field. (b) The recorded signal at two frequencies and fields as a function of the number of field rotations.

7. Conclusions

The spin wave spectra of an array of nanorings provide useful information regarding the internal state of the system, highlighting the potential of the method as an output for computation. MuMax simulations of a 2×2 grid of nanorings showed a changing response in the amplitude of the spin wave spectra as a function of ring state, for a fixed excitation, demonstrating the capability of the microwave response at providing information regarding the transitional regime between onion states orthogonal to the RF excitation to vortex, 3/4 states and onion states parallel to the RF.

Experimental measurements of the microwave response of a NiFe ring array showed three distinct regimes which align with those observed in magnetoresistnce measurements; at low rotating fields the domain walls are pinned, at sufficiently high fields they coherently follow the field, and in between these two regimes, the stochastic interactions at the junctions between rings lead to a plethora of different state alignments which alter the high frequency response. This nonlinear behavior in the measured output fulfils one of the criteria for RC. Furthermore, the response to an input stimulus is not instantaneous, multiple cycles of field are required to achieve a steady-state response, fulfilling the second criteria for RC, a 'fading memory'. We believe these results highlight the capability of the spin wave spectra to provide a multi-dimensional output for nanoring arrays, which may greatly increase their computational capability.

Acknowledgments

We acknowledge funding from the Horizon 2020 FET-Open SpinEngine (Agreement No. 861618) and the EPSRC MARCH project EP/V006339/1 and EP/V006029/1. The data that support the findings of this study are openly available at https://doi.org/10.15131/shef.data.26947465.

ORCID

C. Swindells https://orcid.org/0000-0002-9572-5930
D. R. Eade https://orcid.org/0009-0004-8277-2908
T. J. Hayward https://orcid.org/0000-0002-3732-3095

References

1. N. K. Upadhyay, H. Jiang, Z. Wang, S. Asapu, Q. Xia and J. Joshua Yang, *Adv. Mater. Technol.* **4**, 1800589 (2019).
2. H. Jaeger, Bonn, Germany: German National Research Center for Information Technology GMD, Technical Report No. 148 (2001).
3. M. Lukoševičius, H. Jaeger and B. Schrauwen, *KI-Künstliche Intelligenz* **26**, 365 (2012).
4. G. Indiveri, B. Linares-Barranco, R. Legenstein, G. Deligeorgis and T. Prodromakis, *Nanotechnology* **24**, 384010 (2013).
5. Y. Zhong, J. Tang, X. Li, B. Gao, H. Qian and H. Wu, *Nat. Commun.* **12**, 408 (2021).
6. K. Vandoorne, W. Dierckx, B. Schrauwen, D. Verstraeten, R. Baets, P. Bienstman and J. Van Campenhout, *Opt. Express* **16**, 11182 (2008).
7. K. Vandoorne, P. Mechet, T. Van Vaerenbergh, M. Fiers, G. Morthier, D. Verstraeten, B. Schrauwen, J. Dambre and P. Bienstman, *Nat. Commun.* **5**, 3541 (2014).
8. A. Welbourne, A. Levy, M. Ellis, H. Chen, M. Thompson, E. Vasilaki, D. Allwood and T. Hayward, *Appl. Phys. Lett.* **118**, 012403 (2021).
9. D. A. Allwood *et al.*, *Appl. Phys. Lett.* **122**, 140501 (2023).
10. J. Torrejon *et al.*, *Nature* **547**, 428 (2017).
11. T. Kanao, H. Suto, K. Mizushima, H. Goto, T. Tanamoto and T. Nagasawa, *Phys. Rev. Appl.* **12**, 024052 (2019).
12. D. Prychynenko, M. Sitte, K. Litzius, B. Krüger, G. Bourianoff, M. Kläui, J. Sinova and K. Everschor-Sitte, *Phys. Rev. Appl.* **9**, 014034 (2018).
13. D. Pinna, G. Bourianoff and K. Everschor-Sitte, *Phys. Rev. Appl.* **14**, 054020 (2020).
14. J. H. Jensen, E. Folven and G. Tufte, Computation in artificial spin ice, *ALIFE 2018: Conference on Artificial Life: Beyond AI*, (2018), p. 15–22.
15. J. C. Gartside, K. D. Stenning, A. Vanstone, H. H. Holder, D. M. Arroo, T. Dion, F. Caravelli, H. Kurebayashi and W. R. Branford, *Nat. Nanotechnol.* **17**, 460 (2022).
16. R. V. Ababei, M. O. Ellis, I. T. Vidamour, D. S. Devadasan, D. A. Allwood, E. Vasilaki and T. J. Hayward, *Sci. Rep.* **11**, 15587 (2021).
17. R. W. Dawidek *et al.*, *Adv. Funct. Mater.* **31**, 2008389 (2021).
18. I. T. Vidamour *et al.*, *Nanotechnology* **33**, 485203 (2022).
19. I. Vidamour *et al.*, *Commun. Phys.* **6**, 230 (2023).
20. G. Venkat *et al.*, *Neuromorphic Comput. Eng.* **5**, 024018 (2024).
21. R. Nakane, G. Tanaka and A. Hirose, *IEEE Access* **6**, 4462 (2018).

22. A. Papp, G. Csaba and W. Porod, *Appl. Phys. Lett.* **119**, 052107 (2021).
23. K. D. Stenning, J. C. Gartside, L. Manneschi, C. T. Cheung, T. Chen, A. Vanstone, J. Love, H. Holder, F. Caravelli and H. Kurebayashi, *Nat. Commun.* **15**, 7377 (2024).
24. C. Tian, U. Chaudhuri, N. Singh and A. O. Adeyeye, *Nanotechnology* **31**, 145714 (2020).
25. D. Tripathy and A. Adeyeye, *J. Appl. Phys.* **105**, 07D703 (2009).
26. Y. Ren, N. Singh and A. Adeyeye, *J. Appl. Phys.* **113**, 163903 (2013).
27. A. Vansteenkiste, J. Leliaert, M. Dvornik, M. Helsen, F. Garcia-Sanchez and B. Van Waeyenberge, *AIP Adv.* **4**, 107133 (2014).
28. J. Leliaert, B. Van de Wiele, A. Vansteenkiste, L. Laurson, G. Durin, L. Dupré and B. Van Waeyenberge, *J. Appl. Phys.* **115**, 17D102 (2014).
29. C. A. Vaz *et al.*, *J. Phys.: Condens. Matter* **19**, 255207 (2007).
30. F. Castano, C. Ross, C. Frandsen, A. Eilez, D. Gil, H. I. Smith, M. Redjdal and F. Humphrey, *Phys. Rev. B* **67**, 184425 (2003).
31. T. Hayward, *Sci. Rep.* **5**, 13279 (2015).
32. C. Kittel, *Phys. Rev.* **73**, 155 (1948).